ABCG1 and ABCG4 are coexpressed in neurons and astrocytes of the CNS and regulate cholesterol homeostasis through SREBP-2

Paul T. Tarr* **and Peter A. Edwards**[1,*,†,§]

Departments of Biological Chemistry* and Medicine,[†] David Geffen School of Medicine, and Molecular Biology Institute,[§] University of California at Los Angeles, Los Angeles, CA 90095

Abstract **Here, we describe the initial characterization of *Abcg4*$^{-/-}$ mice and identify overlapping functions of ABCG4 and ABCG1 in the brain. Histological examination of tissues from *Abcg4*$^{+/-}$*/nlsLacZ* and *Abcg1*$^{+/-}$*/nlsLacZ* mice demonstrates that coexpression of *Abcg4* and *Abcg1* is restricted to neurons and astrocytes of the central nervous system (CNS). Interestingly, *Abcg4* mRNA is undetectable outside the CNS, in contrast with the broad tissue and cellular expression of *Abcg1*. We also used primary astrocytes, microglia, neurons, and macrophages to demonstrate that the expression of *Abcg1*, but not *Abcg4*, is induced after the activation of liver X receptor. Cellular localization studies demonstrated that both proteins reside in RhoB-positive endocytic vesicle membranes. Furthermore, overexpression of either ABCG1 or ABCG4 increased the processing of sterol-regulatory element binding protein 2 (SREBP-2) to the transcriptionally active protein, thus accounting for the observed increase in the expression of SREBP-2 target genes and cholesterol synthesis. Consistent with these latter results, we show that the expression levels of the same SREBP-2 target genes are repressed in the brains of *Abcg1*$^{-/-}$ and, to a lesser extent, *Abcg4*$^{-/-}$ mice. Based on the results of the current study, we propose that ABCG1 and ABCG4 mediate the intracellular vesicular transport of cholesterol/sterols within both neurons and astrocytes to regulate cholesterol transport in the brain.**—Tarr, P. T. and P. A. Edwards. **ABCG1 and ABCG4 are coexpressed in neurons and astrocytes of the CNS and regulate cholesterol homeostasis through SREBP-2.** ***J. Lipid Res.*** **2008.** 49: **169–182.**

Supplementary key words liver X receptor • ATP binding cassette transporters G1 and G4 • sterol-regulatory element binding protein 2 • central nervous system

ABC transporters G1 and G4 are two members of a large evolutionarily conserved superfamily of transmembrane proteins that are responsible for the translocation of a diverse array of compounds across specific cellular membrane bilayers that include the endoplasmic reticulum, mitochondria, peroxisomes, and plasma membrane (1, 2). In contrast to all other ABC transporters, the ABCG family is composed solely of half-transporters that have a unique structural organization in which the ABC binding cassette is located on the N-terminal side of the transmembrane region. Mammalian ABCG1 (3–5) and ABCG4 (6–8) were originally cloned in 1996 and 2001, respectively, and were found to encode proteins of ~74 kDa that have 69% identity (82% similarity) at the amino acid level. *Abcg1* mRNA has been reported to be broadly expressed in many tissues, including brain, eye, kidney, spleen, lung, liver, and intestine, as a result of its expression in many different cell types, including macrophages, epithelial cells, endothelial cells, and lymphocytes (5, 9, 10). Several studies have reported varying tissue expression patterns for *Abcg4*, wherein the mRNA has been detected in multiple tissues or conversely found only in the brain and eye (6–8, 11).

Initial reports demonstrated that *Abcg1* mRNA levels were highly induced either during the conversion of macrophages to lipid-loaded foam cells or after the activation of the liver X receptor (LXR) (12, 13). More recently, studies using macrophages derived from *Abcg1*$^{-/-}$ mice (10, 14), the knockdown of *Abcg1* mRNA by RNA interference in macrophages (12, 15), or overexpression of ABCG1 in cultured cells (9, 15–19) have all demonstrated that ABCG1 promotes the efflux of cellular cholesterol to exogenous lipid acceptors. These acceptors include HDL, small unilamellar phospholipid vesicles, and phospholipid/apolipoprotein A-I (apoA-I) or apoE complexes but not lipid-poor apoA-I (10, 15–18). In contrast to ABCG1, very little is known about the physiological importance and function of ABCG4. Given the close similarity with ABCG1, most

Abbreviations: apoA-I, apolipoprotein A-I; CA, cornu ammonis; CNS, central nervous system; GFAP, glial fibrillary acidic protein; GFP, green fluorescent protein; LXR, liver X receptor; QPCR, quantitative real-time polymerase chain reaction; SREBP-2, sterol-regulatory element binding protein 2.

[1] To whom correspondence should be addressed.
e-mail: pedwards@mednet.ucla.edu

Manuscript received 14 August 2007 and in revised form 19 September 2007 and in re-revised form 28 September 2007.

Published, JLR Papers in Press, October 4, 2007.
DOI 10.1194/jlr.M700364-JLR200

studies to date have focused on a role for ABCG4 in regulating cholesterol efflux. Engel et al. (11) originally reported that *Abcg4* mRNA was not only expressed in primary human macrophages but the transcript levels were induced by >6-fold after the addition of LXR/retinoid X receptor agonists. In addition, transient overexpression of ABCG4 in various cell types has been shown to increase cholesterol efflux to HDL and/or phospholipid/apoA-I complexes (15, 16). However, the importance of ABCG4 in maintaining macrophage lipid homeostasis is not clear, as cholesterol efflux to HDL_2 from *Abcg4*$^{-/-}$ macrophages was essentially the same as efflux from wild-type control macrophages (14).

Studies performed with *Abcg1*$^{-/-}$ mice revealed a critical role for ABCG1 in maintaining overall lipid homeostasis in the lung. *Abcg1*$^{-/-}$ mice fed a high-fat/high-cholesterol diet for 9 weeks develop a rather remarkable pulmonary lipidosis that is characterized by massive lipid deposition of cholesteryl esters and cholesterol crystals within alveolar macrophages, consistent with a defect in cholesterol efflux from these cells (10). A similar pulmonary phenotype develops in chow-fed *Abcg1*$^{-/-}$ mice by 6 months (20). These latter studies identified a potentially important role for ABCG1 in the surfactant-secreting type 2 cells, as it was shown that type 2 cells in the lungs of *Abcg1*$^{-/-}$ mice accumulated enlarged and numerous lamellar bodies and the lungs contained excessive amounts of surfactant (20). Together, these data indicate that ABCG1 has an essential function in controlling overall lipid homeostasis in the lungs of mice and identify a critical role for the ABCG1 protein in type 2 pneumocytes as well as macrophages. In contrast, no detailed study describing the loss of ABCG4 function in mice has been reported to date, with the exception that Wang et al. (14) have shown that there is no significant difference in the rate of cholesterol efflux from *Abcg4*$^{-/-}$ or wild-type mouse macrophages.

Several recent studies have begun to address the possible function of ABCG1 or ABCG4 in the brain. In situ hybridization experiments using adult and fetal brain tissue have shown that both *Abcg4* and *Abcg1* mRNAs are expressed in the same areas of the brain, but the resolution did not allow for the identification of specific cell types that express both transcripts (9, 21). Based on the cell culture model TR-CSFB3, it was proposed that ABCG4 and ABCG1 facilitate cholesterol efflux from the choroid plexus epithelial cells into the cerebrospinal fluid (22). Additional studies with primary rodent astrocytes, or with human astrocytoma or neuroblastoma cell lines, indicate that activation of LXR and its many target genes regulates cholesterol efflux to apoE (23, 24). In addition, overexpression of ABCG1 in Chinese hamster ovary or HEK293 cells was reported not only to increase cholesterol efflux but also to affect the cleavage of stably expressed amyloid precursor protein (25, 26). However, the physiological importance and function of ABCG1 or ABCG4 in regulating cholesterol homeostasis in the central nervous system (CNS) is still poorly understood.

In the current study, we present the first detailed characterization of the *Abcg4*$^{-/-}$ mouse and provide a detailed study of the functions of ABCG4 and ABCG1 in the mouse brain. By analyzing both *Abcg4*$^{+/-}$*/nlsLacZ* and *Abcg1*$^{+/-}$*/nlsLacZ* knockin mice, we found that coexpression of these two ABC transporters is limited to neurons and astrocytes. Furthermore, we show that both proteins are localized within intracellular vesicles of primary neurons and astrocytes. Gain-of-function studies, using adenoviral expression of either ABCG1 or ABCG4 in primary mouse cultures of astrocytes or neurons, result in increased processing of sterol-regulatory element binding protein 2 (SREBP-2), activation of SREBP-2 target genes, and increased cholesterol synthesis. In addition, we show that many of these same SREBP-2 genes are repressed in the brains of *Abcg1*$^{-/-}$ and *Abcg4*$^{-/-}$ mice. To date, these changes in gene expression are the only phenotype we have observed in the CNS of these mice. Together, the results of the current study suggest that ABCG1 and ABCG4 function to regulate intracellular sterol transport in both astrocytes and neurons.

MATERIALS AND METHODS

Cloning of mouse ABCG4 and ABCG1

cDNAs were generated from total mouse brain RNA (C57BL/6 mice) using SuperScript II (Invitrogen). Gene-specific primers were then used to PCR-amplify (Tgo high-fidelity DNA polymerase; Roche) sequences corresponding to the open reading frames for ABCG1 and ABCG4. The PCR products were TOPO TA-cloned (Invitrogen), sequenced, and found to match the known Refseqs for ABCG1 (NM_009593) and ABCG4 (NM_138955). The amino acid sequence of the cloned ABCG1 corresponds to that encoded by *Abcg1-a* mRNA, previously reported by Nakamura et al. (9). Expression plasmids were generated by subcloning the cDNAs for *Abcg1* and *Abcg4* into the *Hind*III/*Bam*HI sites or the *Nhe*I/*Hind*III sites of pcDNA3.1 (+) (Invitrogen), respectively. A tandem three copy sequence of either the Hemagglutinin (HA) or the Flag epitope was inserted in-frame into 3′ cloning sites (*Bam*HI or *Hind*III) of the pcDNA3.1-mABCG1 or pcDNA-mABCG4 to give pcDNA3.1-mABCG1-HA or -Flag and pcDNA3.1-mABCG4-HA or -Flag. All other constructs reported in this study were generated from these original clones.

Production of adenovirus

Adenovirus was produced using the pAdEasy Adenoviral Vector System (Stratagene) by cloning the cDNA for ABCG1-Flag or ABCG4-Flag into the *Bgl*II/*Xho*I sites of pShuttle-IRES-GFP (for green fluorescent protein). The corresponding pShuttle-mABCG1-Flag and pShuttle-mABCG4-Flag plasmids were recombined with pAdEasy-1 according to the manufacturer's protocol. Recombinants were identified by the presence of a 3.0 or a 4.5 kb *Pac*I fragment. Three independent recombinant plasmids for both ABCG1-Flag and ABCG4-Flag were transfected individually into the Ad293 cell line (Stratagene) for the production and amplification of adenovirus. Adenoviruses were purified by CsCl gradient ultracentrifugation, and the titers were calculated to be 1×10^{11} plaque-forming units/ml for Ad-GFP, 8×10^{10} plaque-forming units/ml for Ad-ABCG1-Flag, and 5×10^{10} plaque-forming units/ml for Ad-ABCG4-Flag.

Mice

Abcg1$^{-/-}$*/nlsLacZ* mice, containing the LacZ gene modified to contain a nuclear targeting signal (nls), have been described

previously (10, 20). The LacZ/neo cassette was inserted into the Walker A motif in exon 3 of the *Abcg1* gene. Thus, expression of the LacZ gene is controlled by all three endogenous mouse *Abcg1* promoters (9). In addition, the presence of a strong splice acceptor site in the LacZ/neo cassette ensures that all transcripts initiating from the *Abcg1* gene are spliced into the LacZ locus. The result is that β-galactosidase activity is a measure of the transcriptional activity of all three *Abcg1* promoters.

The *Abcg4*$^{+/-}$/*nlsLacZ* mice on a C57BL/6 background (seven backcrosses) were obtained from Deltagen, Inc. (San Carlos, CA). Bases 1,622 to 1,647 of *Abcg4* (Refseq NM_138955) were targeted with a Neo-IRES-nlsLacZ-cassette. *Abcg4*$^{-/-}$ mice were generated by crossing of the *Abcg4*$^{+/-}$ mice. All animal work was performed following National Institutes of Health guidelines, with all protocols approved by the Animal Resources Committee at the University of California, Los Angeles.

Histology and β-galactosidase staining

Anesthetized mice were intracardially perfused via the left ventricle with PBS (pH 7.4) followed by 4% paraformaldehyde/0.1 M phosphate buffer (pH 7.4) for 10 min. The brain was removed and fixed for an additional 4 h at 4°C in 4% paraformaldehyde/0.1 M phosphate buffer (pH 7.4). Cryoprotection, sectioning, and β-galactosidase staining of tissue were performed as described previously (10). For whole-mount tissue staining, brains were removed and fixed in paraformaldehyde as described above. The whole tissue was then submerged in β-galactosidase staining buffer for 16 h and stained as described (10).

RNA isolation and quantitative real-time polymerase chain reaction

RNA was isolated using Trizol Reagent (Invitrogen) (10). One microgram of DNaseI-treated RNA was used to generate cDNA using SuperScript II and random hexamer primers (Invitrogen). Quantification of *Abcg1* and *Abcg4* mRNAs in primary macrophages was performed using gene-specific FAM-labeled Taqman probes and IQ Supermix (Bio-Rad). All other quantitative real-time polymerase chain reactions (QPCRs) were performed using the IQ Sybr Green Supermix (Bio-Rad) as described (10). GAPDH was used as an internal control for mRNA quantification. Data obtained from the MyiQ Real-Time PCR detection system (Bio-Rad) were analyzed as described previously (10). Primer and probe sequences are available upon request.

Isolation of mouse peritoneal macrophages and human monocyte-macrophages

Thioglycollate-elicited mouse peritoneal macrophages (10) and primary human monocyte-macrophages were obtained and cultured for 4 and 8 days as described previously (13).

Isolation of primary mouse astrocytes, hippocampal neurons, and microglia

Brains were dissected from P0 C57BL/6 pups, the meninges were carefully removed, and the tissue was cut into small pieces before incubation in 0.05% trypsin/DMEM-F12 (1:1) for 30 min at 37°C. A cell suspension was generated by triturating the tissue 15–20 times with a large-bore glass pipette. Cells were pelleted (1,000 *g* for 10 min) and resuspended in DMEM/F-12 (1:1) (Invitrogen) containing 20% FBS, 15 mM HEPES, 2.4 g/L sodium bicarbonate, and 1% penicillin/streptomycin (astrocyte growth medium). Cells obtained from multiple brains were pooled and plated on 100 mm cell culture dishes (Corning).

Primary astrocyte and microglia cultures were obtained by the method described by Saura, Tusell, and Serratosa (27). Briefly, the astrocyte monolayer was separated from the microglia by mild trypsinization (0.125% trypsin in 1:1 DMEM/F-12 medium with no serum) for 10–15 min until the astrocyte monolayer detached. The detached astrocytes were collected and pelleted by centrifugation at 50 *g* for 5 min at 4°C. New culture medium (astrocyte growth medium) was added and the cells were plated onto dishes/wells. After removal of the astrocyte monolayer, the microglia (which remain attached to the culture dish during the trypsin step) were refreshed with the original culture medium that had been collected and sterile-filtered through a 0.45 μm filter (Millipore GP express plus membrane) before separation of the astrocytes. Astrocytes and microglia isolated by this technique are >95% pure, as determined by staining for glial fibrillary acidic protein (GFAP). For gene expression studies, cells were incubated in medium containing 10% FBS after infection with adenovirus or before the addition of LXR agonist.

Primary hippocampal neuron cultures were obtained from P0 C57BL/6 pups. The hippocampi were digested in 1.25 U/ml papain (Sigma) in L-15 medium (Gibco) for 30 min at 30°C and then washed twice in L-15 medium containing 1xB27 supplement (Gibco) to remove residual papain. The tissue was triturated (15–20 times) with a large-bore glass pipette, and the resulting single cells were suspended in Neurobasal-A+ medium supplemented with 5% equine serum, 1xB27 supplement, 0.5 mM glutamax (Gibco), FDU (21.4 μg/ml uridine and 8.7 μg/ml 5-fluoro-deoxy-uridine), and 1% penicillin/streptomycin. Cells (50,000–60,000 per well) were plated onto poly-L-lysine glass cover slips in 24-well dishes and used after 8–12 days. Where indicated, primary astrocytes and hippocampal neurons were infected with Ad-GFP, Ad-ABCG1-Flag, or Ad-ABCG4-Flag (1×10^7 plaque-forming units/ml culture medium) for 24 h before isolation of RNA or processing for immunofluorescence.

Cholesterol synthesis and cholesterol efflux

Astrocytes, plated onto six-well plates, were infected with 1×10^7 plaque-forming units/ml control Ad-GFP, Ad-ABCG1-Flag, or Ad-ABCG4-Flag. After 24 h, cells were washed twice with PBS to remove residual viral particles, and fresh astrocyte growth medium supplemented with 10% FBS and 1.67 μCi/ml [^{14}C]sodium acetate (Sigma) was added to cells. After 4 h, cells were washed three times with PBS and then incubated at 4°C with 2 ml of isopropanol containing 50,000 dpm [^{3}H]cholesterol. After 24 h, isopropanol was recovered, cleared of cell debris, and evaporated at 55°C under nitrogen. Lipids were saponified in 70% ethanol/1 N NaOH and hydrolyzed by incubation at 60°C for 1 h. Neutral lipids were extracted into hexane and lipids separated using thin-layer chromatography (Whatman) with a solvent system of 146:50:4 (v/v) hexane-ether-acetic acid. The band corresponding to cholesterol was recovered, and the radioactive content (^{3}H and ^{14}C) was determined by scintillation counting. The [^{14}C]cholesterol levels were corrected for recovery using the [^{3}H]cholesterol internal standard, and the synthesis of [^{14}C]cholesterol was determined as dpm/mg cell protein/4 h.

Cholesterol efflux experiments from infected astrocytes were performed as described previously (20). Briefly, mouse primary astrocytes in quadruplicate were incubated in medium supplemented with 0.2% BSA containing [^{3}H]cholesterol (2 μCi/ml) for 24 h. The cells were then washed and incubated in medium devoid of cholesterol for 1 h. Finally, fresh medium containing 0.2% BSA in the absence or presence of human HDL (50 μg/ml) was added, and the efflux of [^{3}H]cholesterol to the medium was determined over a 4 h period. Percentage efflux was determined by dividing the [^{3}H]cholesterol content of the medium by the [^{3}H]cholesterol content of the medium plus cells.

Immunostaining and confocal microscopy

Primary neurons and astrocytes were infected with adenovirus as described above. After 24 h, cells were processed for immunofluorescence studies by fixation in 3.7% formaldehyde in PBS (pH 7.4) for 10 min, followed by treatment with 0.18% Triton X-100 in PBS (pH 7.4) for 10 min and then 50 mM NH_4Cl for 10 min. Cover slips were subsequently treated for 30 min in blocking buffer (5% normal goat serum and 1% BSA in TBS, pH 7.4) before the cells were costained for 1 h at room temperature with antibodies to Flag (Sigma; rabbit polyclonal) and Tau (Chemicon; clone PC1C6) or Map2 (Sigma; clone HM2) or synaptophysin (Chemicon; MAB5258) diluted 1:500 in blocking buffer. The cells/cover slips were washed three times in PBS (5 min each) before the addition of anti-rabbit Alexa-546 and anti-mouse Alexa-633 conjugated secondary antibodies (Molecular Probes) diluted 1:500 in blocking buffer. After 30 min at room temperature, the cells were washed three more times with PBS and mounted onto slides (Fisher; Superfrost plus glass slides) using prolong gold antifade reagent (Molecular Probes).

Cos-7 cells were transfected (500 ng DNA/well) at ~70% confluence using Lipofectamine 2000 (Invitrogen) and seeded onto poly-L-lysine (Sigma)-treated glass cover slips (Fisher). After 18 h, cells were fixed and processed as described above. Cover slips were subsequently treated with blocking buffer for 30 min, followed by incubation with the HA.11 (Covance) antibodies or Flag (Sigma) antibodies (diluted 1:500 in blocking buffer) for 1 h, and then washed three times in PBS (pH 7.4). Anti-mouse Alexa-488 (Molecular Probes) or anti-rabbit Alexa-594 (Molecular Probes) conjugated secondary antibodies in blocking buffer (1:500 dilution) were added for 1 h at room temperature, and the cells were washed three times in PBS and mounted with prolong gold antifade reagent (Molecular Probes).

For colocalization studies, cells were cotransfected with pAc-RhoB-GFP and ABCG1-HA or ABCG4-Flag using Lipofectamine 2000. All images were taken on a Zeiss confocal microscope with an LSM 5 Pascal laser module at 63× magnification.

Western blot analysis

Primary mouse astrocytes were infected with the adenovirus expressing GFP, or either Flag-tagged ABCG1 or ABCG4, or treated with 1 μM of the LXR agonist GW3965, or DMSO vehicle. The cells were treated and cultured under identical conditions as those used for the gene expression studies described above.

To assess SREBP-2 maturation, cell lysates were prepared as described by Radhakrishnan et al. (28). Proteins (50 μg) were separated using SDS-PAGE and transferred to a polyvinylidene difluoride membrane. Both the precursor and nuclear forms of SREBP-2 were detected by Western blot with an antibody generated against amino acids 812–975 (Santa Cruz; SREBP-2 H-164) diluted 1:250 in 1× TBS containing 0.05% Tween 20 and 5% nonfat dried milk. Immune complexes were detected with anti-rabbit HRP-conjugated secondary antibodies (Bio-Rad) diluted 1:10,000.

To compare the relative protein expression levels after GW3965 treatment or adenovirus transduction, cell lysates were prepared by scraping cell monolayers in 20 mM HEPES, pH 7.4, 0.15 M NaCl, 0.2 mM EDTA, 0.2 mM $MgCl_2$, and 1% Triton X-100 supplemented with a protease inhibitor cocktail (Roche; Complete protease inhibitor tablets). Ten micrograms of protein was separated on a 10% SDS-PAGE gel, and Western blot analysis was performed as described above. ABCG1 (74 kDa) was detected by antibodies raised against a peptide sequence between amino acids 300–400 (Novus; ABCG1 antibody NB400-132) at a dilution of 1:500 in 1× TBS containing 0.05% Tween 20 and 5% nonfat dried milk. To detect Flag-tagged protein (78 kDa), the anti-Flag M2 monoclonal antibody (Sigma) was used at a 1:1,000 dilution in 1× TBS containing 0.05% Tween 20 and 5% nonfat dried milk.

Statistics

Statistical analysis was determined by two-tailed Student's *t*-test.

RESULTS

Abcg1 and *Abcg4* are coexpressed in neurons and astrocytes of the mouse CNS

To identify those tissues and cell types that express both ABCG1 and ABCG4, we used *Abcg1*$^{+/-}$/*nlsLacZ* and *Abcg4*$^{+/-}$/*nlsLacZ* knockin mice. Importantly, β-galactosidase tagged with a nuclear localization sequence is under the control of the endogenous promoter of either the *Abcg1* or *Abcg4* gene, allowing for facile identification of cells that express ABCG1 or ABCG4.

Staining of multiple tissue sections indicated that overlapping β-galactosidase activity was only observed in the brain and retina of *Abcg4*$^{+/-}$ and *Abcg1*$^{+/-}$ mice (**Fig. 1A**) (data not shown). Gross examination of the β-galactosidase-stained brains indicated that *Abcg1* and *Abcg4* were both expressed in gray and white matter (Fig. 1A). Surprisingly, β-galactosidase expression was undetectable in any tissue outside the CNS of *Abcg4*$^{+/-}$ mice, including the macrophage- and lymphocyte-rich spleen (Fig. 1A) (data not shown). In contrast, many tissues, including the spleens of *Abcg1*$^{+/-}$ mice, expressed β-galactosidase (Fig. 1A) (10). As expected, β-galactosidase activity was not detected in tissues of control wild-type C57BL/6 mice (Fig. 1A).

The brain is a complex tissue that is composed primarily of two major cell types, glial cells and neurons. Astrocytes, microglia, and oligodendrocytes represent glial cells that make up ~90% of all of the cells present in the brain. The vast majority of the remaining cells in the brain are composed of various classes of highly specialized neurons (29). To identify which of these cell types express *Abcg1* and *Abcg4*, sagittal brain sections obtained from *Abcg1*$^{+/-}$ and *Abcg4*$^{+/-}$ mice were assayed for β-galactosidase activity (Fig. 1B). Detailed comparison of these stained tissue sections revealed that many different classes of neurons express both *Abcg1* and *Abcg4*. Figure 1B shows that β-galactosidase-positive neurons include mitral cells and neurons of the glomeruli in the olfactory bulbs, the pyramidal cells in the cornu ammonis (CA) regions of the hippocampus, the granule cell neurons of the dentate gyrus, and Purkinje cells and granule cell neurons in the cerebellum of both genotypes. Interestingly, the granule cells of both the cerebellum and the olfactory bulb show greater staining intensity for β-galactosidase in *Abcg1*$^{+/-}$ mice compared with *Abcg4*$^{+/-}$ mice [Fig. 1B, compare areas denoted gr (granule cells) in the cerebellum and olfactory bulb panels]. Expression of β-galactosidase was also observed in neurons of the striatum and the cortex (Fig. 1B). In addition, β-galactosidase was also observed in scattered GFAP-positive astrocytes of both genotypes, as assessed by costaining with antibodies to β-galactosidase and GFAP (data not shown).

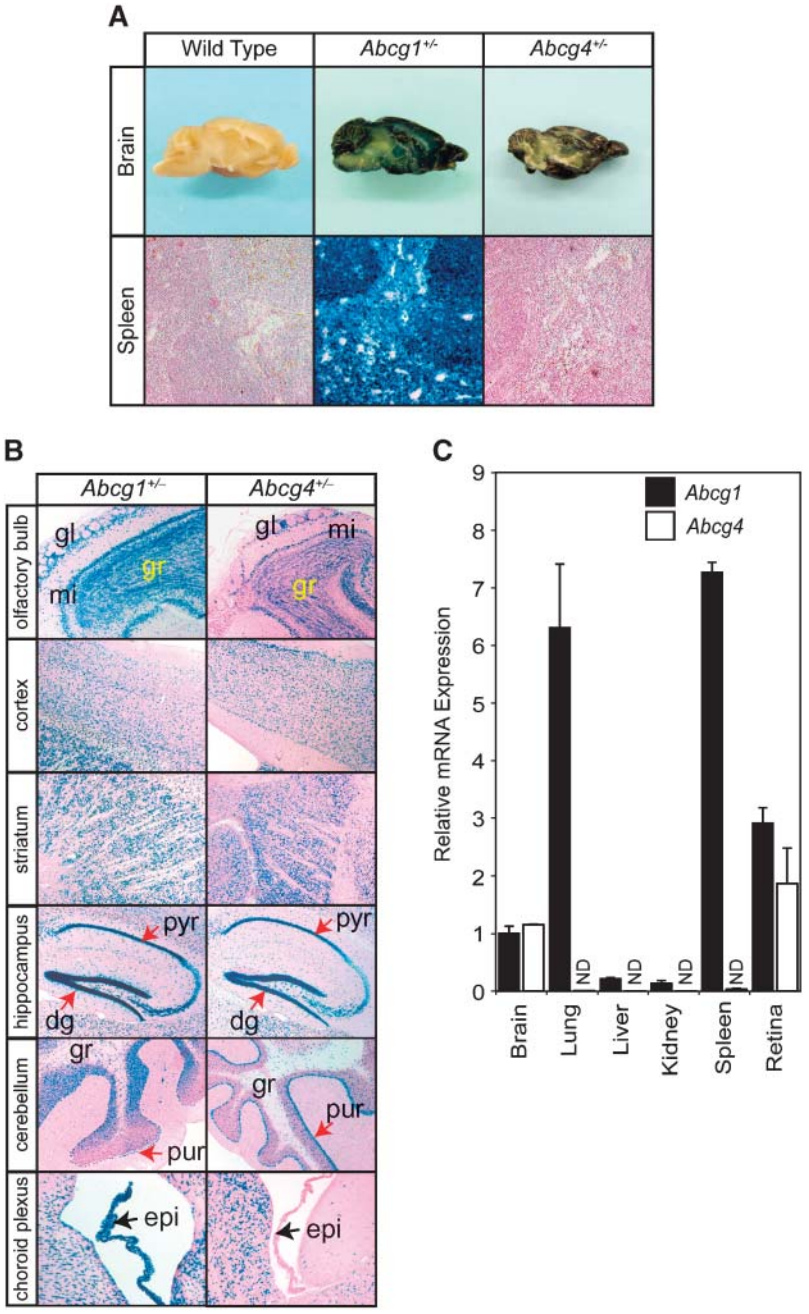

Fig. 1. *Abcg1* and *Abcg4* are coexpressed in the same types of neurons. A: Brains and spleens of chow-fed 3 month old mice of the indicated genotypes were stained for β-galactosidase activity. B: Serial sagittal sections from the brains of $Abcg1^{+/-}$ and $Abcg4^{+/-}$ mice were stained for β-galactosidase activity. Glomeruli (gl), mitral cell layer (mi), granule cell layer (gr) of the olfactory bulbs, the pyramidal neurons (pyr) of the CA regions of the hippocampus, the granule cell neurons of the dentate gyrus (dg), the Purkinje cells (pur) and granule cell (gr) neurons of the cerebellum, and the epithelial cells (epi) of the choroid plexus are indicated. C: Quantification by quantitative real-time polymerase chain reaction (QPCR) of *Abcg1* and *Abcg4* mRNA in the indicated mouse tissues. GAPDH was used as the internal control for all tissues. Values are represented as mean ± SEM. ND, not detectable.

One striking discrepancy in the expression between the two genotypes was observed in the epithelial cells of the choroid plexus. β-Galactosidase activity was high in the epithelial cells of $Abcg1^{+/-}$ mice but was undetectable in the corresponding cells of $Abcg4^{+/-}$ mice (Fig. 1B). These data are consistent with the expression of β-galactosidase in epithelial cells of the lung, liver, and kidney of $Abcg1^{-/-}$ mice (10) and the lack of expression of β-galactosidase in these same cells of $Abcg4^{+/-}$/*nlsLacZ* mice (data not shown).

We also used QPCR to quantify the relative endogenous expression of *Abcg1* and *Abcg4* mRNAs in multiple tissues of C57BL/6 mice. The data in Fig. 1C show that, in contrast to *Abcg1* mRNA, which is detected in multiple tissues, including brain, retina, lung, liver, kidney, and spleen, *Abcg4* mRNA expression is limited to the brain and retina and is undetectable in tissues such as the lung, liver, kidney, and spleen. Thus, the mRNA expression data are entirely consistent with the results obtained after β-galactosidase staining of tissues from $Abcg4^{+/-}$/*nlsLacZ* and $Abcg1^{+/-}$/*nlsLacZ* mice (Fig. 1A, B). We conclude that the expression of ABCG4 is limited to the cells of the brain and retina and that ABCG1 is expressed in multiple tissues, including cells of the CNS.

Expression of *Abcg1*, but not *Abcg4*, is regulated by LXR

Previous studies have shown that ligand activation of LXR results in the increased expression of *Abcg1* in multiple cell types, including macrophages, astrocytes, and

neurons (23, 25, 30, 31). *Abcg4* has also been reported to be induced in macrophages after the activation of LXR (11). To determine whether LXR regulates *Abcg4* mRNA expression in the different cell types of the brain, we incubated primary cultures of neurons, astrocytes, or microglia from wild-type mice with either vehicle or the LXR agonist GW3965 for 24 h before the isolation of RNA. The data in **Fig. 2** demonstrate that the basal expression of *Abcg1* and *Abcg4* mRNAs is ~5-fold higher in neurons compared with astrocytes, consistent with the higher levels of β-galactosidase activity in neurons of brain sections from $Abcg1^{+/-}$ and $Abcg4^{+/-}$ mice (Fig. 1B). The basal expression level for *Abcg1* in microglia (Fig. 2C) is approximately equivalent to the mRNA levels observed in neurons (Fig. 2A). Interestingly, *Abcg4* mRNA was not detected in primary mouse microglial cells (Fig. 2C). Activation of LXR by GW3965 resulted in significant induction of *Abcg1* mRNA in neurons, astrocytes, and microglia (Fig. 2A–C). In contrast, *Abcg4* mRNA levels in neurons or astrocytes were unaffected by GW3965 treatment (Fig. 2A, B) and remained undetectable in primary microglial cells (Fig. 2C).

To rule out the possibility that the induction of *Abcg4* mRNA by LXR is macrophage-specific, isolated primary mouse and human macrophages were treated with vehicle or GW3965 for 24 h. In agreement with numerous other studies, LXR activation resulted in robust induction of *Abcg1* mRNA levels in both mouse and human cells (Fig. 2D, E). In contrast, *Abcg4* mRNA levels were undetectable in primary mouse or human macrophages even after the activation of LXR with GW3965 (Fig. 2D, E). RNA isolated from mouse brain or human retina served as positive controls for the QPCR (Fig. 2D, E). These data unambiguously demonstrate that coexpression of *Abcg1* and *Abcg4* is limited to neurons and astrocytes and that, unlike *Abcg1*, *Abcg4* expression is unchanged after the activation of LXR.

ABCG1 and ABCG4 reside within intracellular vesicles of neurons and astrocytes

To determine the cellular localization of ABCG1 and ABCG4 in neurons and astrocytes, we infected primary mouse neurons and astrocytes with adenovirus-expressing C-terminal Flag-tagged proteins. Importantly, the presence of the C-terminal epitope did not adversely affect

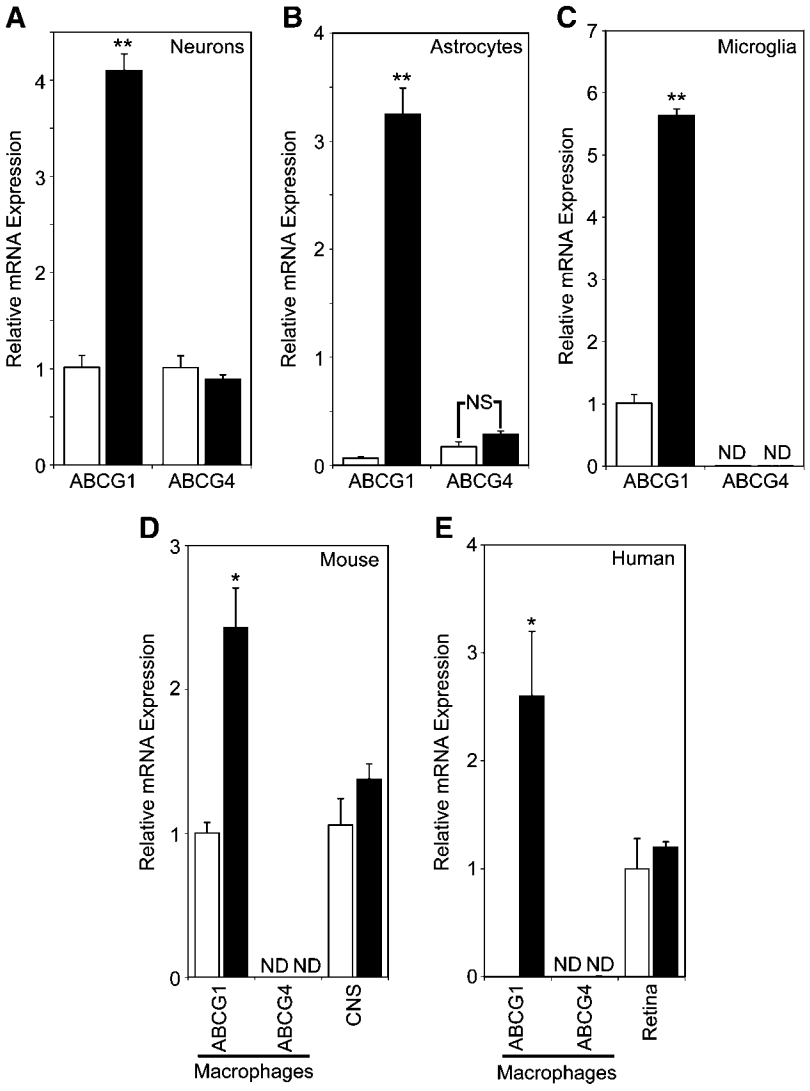

Fig. 2. *Abcg1* and *Abcg4* are differentially regulated by the nuclear receptor liver X receptor (LXR) in primary neurons, astrocytes, microglia, and macrophages. Quantification of *Abcg1* or *Abcg4* mRNA levels by QPCR in mouse hippocampal neurons (A), astrocytes (B), microglia (C), peritoneal mouse macrophages (D), or human monocyte-derived macrophages (E) treated for 24 h with vehicle (open bars) or 1 μM GW3965 (closed bars), a synthetic LXR agonist. Values are represented as means ± SEM from multiple primary hippocampal neuronal (n = 6), astrocyte (n = 3), and microglial (n = 3) cultures and are representative of two independent experiments. The cycle threshold (Ct) value for *Abcg1* mRNA in the vehicle-treated hippocampal neuron was the reference that all other samples were compared with in A–C to determine relative expression levels. RNA from mouse brain or human retina served as positive controls for the QPCR in D and E. * $P < 0.05$, ** $P < 0.001$. ND, not detected; NS, not significant.

function, as determined by a cholesterol efflux assay from HEK293 cells to HDL (data not shown).

Immunostaining of infected neurons with anti-Flag antibody demonstrated that both ABCG1 and ABCG4 were present in intracellular vesicles (**Fig. 3A**). Costaining with antibodies to Tau, a microtubule-associated protein, indicated that the majority of the punctated Flag-positive vesicles were present in neuronal processes and the cell body (Fig. 3A). Relatively few of the ABCG1-positive vesicles were identified within Map2-positive dendritic processes (Fig. 3B), suggesting that in the steady state most of the ABCG1-positive vesicles are found in axons of neurons. Furthermore, costaining of infected neurons with antibodies to Flag and synaptophysin, a marker for presynaptic vesicles, identified two distinct nonoverlapping vesicle populations, indicating that ABCG1 does not reside on presynaptic vesicle membranes (Fig. 3C). Preliminary results indicate that epitope-tagged ABCG4, like ABCG1,

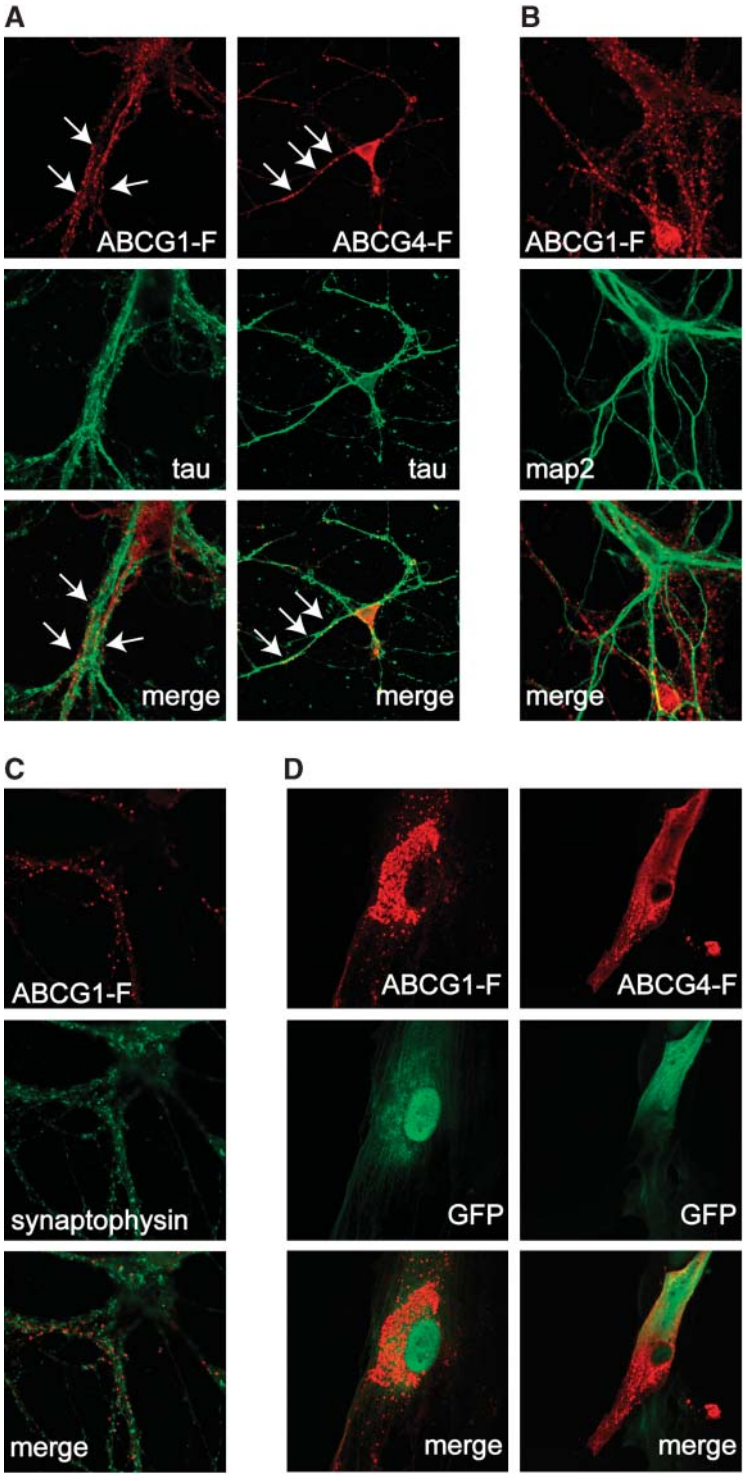

Fig. 3. ABCG1 and ABCG4 are detected in intracellular vesicles in primary mouse hippocampal neurons and primary mouse astrocytes. A: Confocal images of primary hippocampal neurons infected with adenoviruses expressing ABCG1-Flag (ABCG1-F) or ABCG4-Flag (ABCG4-F) were costained with antibodies against Flag (red) and Tau (green). Both proteins localized to vesicles (white arrows) within Tau-positive neuronal processes. B, C: Costaining primary hippocampal neurons with antibodies to Flag (red) and the dendritic microtubule protein Map2 (green) (B) or synaptophysin (green), a marker for presynaptic vesicles (C). D: A similar vesicular staining pattern was observed in primary mouse astrocytes infected with adenoviruses expressing ABCG1-Flag or ABCG4-Flag. Only infected (GFP-positive) cells stained with antibodies to Flag (merge). All images were taken at 63× magnification.

does not colocalize to MAP-2 processes or synaptophysin-positive presynaptic vesicles (data not shown).

Similar localization studies were performed using primary mouse astrocytes infected with adenovirus expressing epitope-tagged ABCG1 and ABCG4. Confocal microscopy localized both ABCG1 and ABCG4 to intracellular vesicles in the infected (GFP-positive) cells (Fig. 3D). These data indicate that in the steady state both ABCG1 and ABCG4 reside in intracellular vesicles in primary astrocytes and hippocampal neurons. Neither protein was detected on the plasma membrane of either cell type.

ABCG1 and ABCG4 reside in the same endosomes

To determine whether ABCG1 and ABCG4 colocalize to the same vesicles, we transiently transfected Cos-7 cells with expression plasmids for HA-tagged ABCG1 (ABCG1-H) and Flag-tagged ABCG4 (ABCG4-F). Immunostaining with antibodies to Flag and HA shows that both epitope-tagged proteins are present intracellularly and exhibit a distinct punctated vesicular pattern (**Fig. 4A**). When the fluorescence signals are merged, the majority of ABCG1- and ABCG4-positive vesicles overlap (Fig. 4A, merge). Additional studies indicate that ABCG1 (Fig. 4B) and ABCG4 (Fig. 4C) colocalize with RhoB-GFP, a marker for endosomes (32). In contrast, neither ABCG1 nor ABCG4 colocalized with antibodies that specifically recognize the Golgi, endoplasmic reticulum, or lysosomes (data not shown). Based on these data, we conclude that ABCG1 and ABCG4 reside within the same population of vesicles in the endosomal pathway.

ABCG1 and ABCG4 regulate SREBP-2 maturation and cholesterol biosynthesis in astrocytes and neurons

The demonstration that ABCG1 and ABCG4 are found on intracellular vesicles, together with the data supporting a role for these two proteins in cholesterol efflux, suggested that these proteins might facilitate the vesicular transport of sterols. To identify those pathways that are affected by

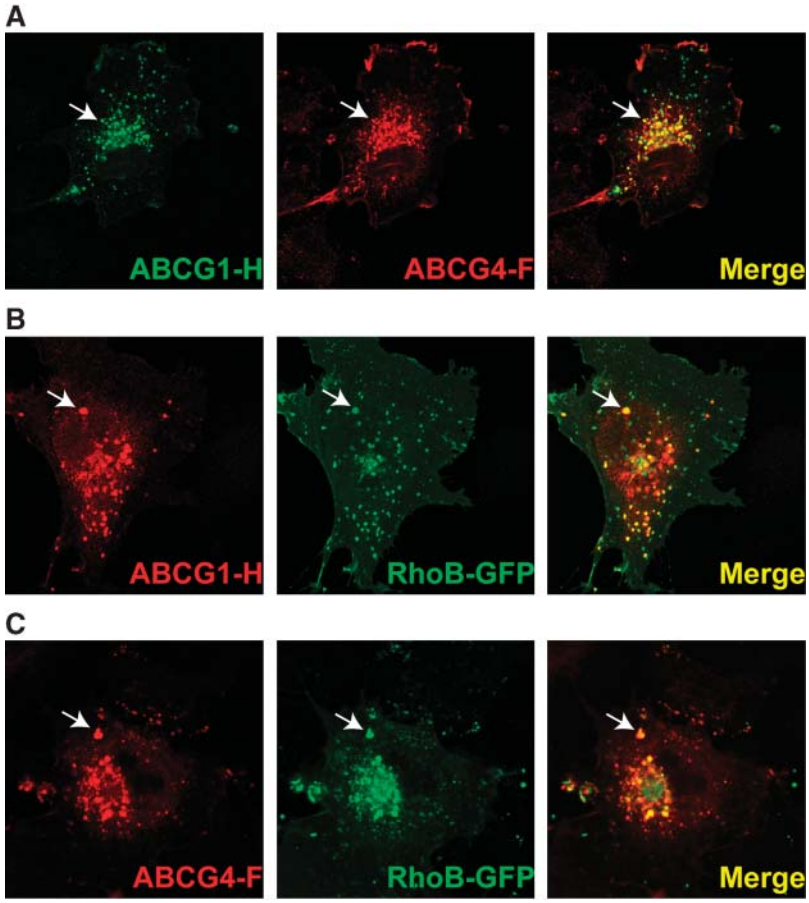

Fig. 4. ABCG1-Flag and ABCG4-Flag are detected in the same endosomes in Cos-7 cells. A: Cos-7 cells were cotransfected with plasmids encoding ABCG1-HA (ABCG1-H) and ABCG4-Flag (ABCG4-F). Transfected cells were costained with antibodies against HA (green) or Flag (red). The last panel shows the merged image of the green and red channels, and white arrows denote representative vesicles positive for both ABCG1 and ABCG4. B, C: Confocal images of Cos-7 cells cotransfected with ABCG1-HA (ABCG1-H) and RhoB-GFP (B) or ABCG4-Flag (ABCG4-F) and RhoB-GFP (C) and stained with antibodies to HA or Flag. The white arrows mark the representative overlapping signals of the endosomal marker RhoB-GFP with ABCG1-HA (B) or ABCG4-Flag (C) in cotransfected cells. Images were taken at 63× magnification.

ABCG1 and ABCG4, we infected both primary mouse astrocytes and neurons with adenoviruses that express GFP or GFP and either ABCG1-Flag or ABCG4-Flag. RNA was isolated from two independent cell preparations and infections and used to probe gene expression arrays (Illumina Mouse-6 expression BeadChip version 1.1).

Pathway analysis of the microarray data showed that, compared with control cells, expression of either ABCG1 or ABCG4 in astrocytes or neurons caused the induction of many genes involved in cholesterol biosynthesis (data not shown). Gene expression analysis by QPCR validated the microarray data confirming that expression of ABCG1 (**Fig. 5A**) or ABCG4 (Fig. 5B) in astrocytes induced the expression of *Srebp-2* mRNA and SREPB-2 target genes, including HMG-CoA reductase (*Hmgr*), HMG-CoA synthase (*Hmgs*), squalene synthase (*Sqs*), farnesyl diphosphate synthase (*Fpps*), low density lipoprotein receptor (*Ldlr*), *Insig-1*, and *StarD4*, but not *apoER2*, a member of the LDL-related family of receptors (Fig. 5A, B). Furthermore, the expression of *apoE* or the LXR target gene *Abca1* was unaffected in these same samples, demonstrating that the changes observed are specific to SREBP-2 target genes (data not shown). Induction of these genes was unexpected, as the infected cells were cultured in the presence of 10% FBS and thus were exposed to high levels of exogenous cholesterol. Such conditions are known to normally repress the expression and processing of SREBP-2 and the subsequent activation of cholesterogenic genes (33, 34).

To determine whether the changes in gene expression that occur in infected astrocytes were paralleled by changes in cholesterol synthesis, we infected primary mouse astrocytes with adenovirus and after 24 h incubated the cells in medium supplemented with [^{14}C]acetate. Quantification of the [^{14}C]cholesterol synthesized during a 4 h period indicated that ABCG1 and ABCG4 overexpression stimulated cholesterol synthesis by 2.5- and 7-fold, respectively (Fig. 5C, D).

These latter data suggest that the expression of ABCG1 or ABCG4 in astrocytes increases the concentration of the SREBP-2 precursor protein and/or the processed transcriptionally active N-terminal nuclear fragment of SREBP-2. As shown in the upper panel of Fig. 5E, infection of astrocytes with adenovirus expressing either ABCG1 or ABCG4 resulted in a small increase in the SREBP-2 precursor protein (lanes 3, 4 for ABCG1 and lanes 5, 6 for ABCG4) compared with cells expressing GFP alone (lanes 1, 2). The mature nuclear, N-terminal fragment of SREBP-2 was undetectable in astrocytes infected with adenovirus expressing GFP and cultured in medium supplemented with 10% FBS (Fig. 5E, lower panel, lanes 1, 2), consistent with the repression of SREBP-2 processing under these conditions. Upon overexpression of ABCG1 or ABCG4, a robust increase in the level of the nuclear form of the SREBP-2 protein was observed (Fig. 5E, lower panel, lanes 3, 4 for ABCG1 and lanes 5, 6 for ABCG4). The finding that the processing of SREBP-2 was increased so markedly after the expression of either ABCG1 or ABCG4 likely accounts for the relatively small increase in the level of the precursor SREBP-2 in these cells (Fig. 5E, upper panel) as it is rapidly converted into the mature transcriptionally active form. Together, these data provide direct evidence that enhanced expression of either ABCG1 or ABCG4 results in increased processing of SREBP-2 to the mature transcriptional active form.

In Fig. 5F, we compared the expression of ABCG1 protein in mouse astrocytes. The data show that ABCG1 protein is undetectable in cells cultured in medium containing FBS, is highly induced after the activation of LXR, and that adenoviral infection results in a further increase in protein levels. In other studies, we have observed similar supraphysiological levels of expression of epitope-tagged ABCG1 or ABCG4 after transient transfection of cells with plasmids or adenoviral infection (data not shown). The lower panel of Fig. 5F demonstrates that Flag-tagged ABCG1 and ABCG4 proteins are expressed at roughly equal levels after adenoviral infection of astrocytes.

As expected, overexpression of ABCG1-Flag or ABCG4-Flag in astrocytes also results in a small but significant increase in cholesterol efflux to HDL (**Fig. 6A, B**).

The expression of cholesterogenic genes is reduced in the brains of *Abcg1*$^{-/-}$ and *Abcg4*$^{-/-}$ mice

Based on the observation that genes involved in cholesterol homeostasis were specifically induced in primary mouse astrocytes or neurons after overexpression of ABCG1 or ABCG4, we predicted that these same mRNAs might be repressed in the brains of *Abcg1*$^{-/-}$ and *Abcg4*$^{-/-}$ mice. The results in **Fig. 7A** confirm this prediction, as many genes involved in cholesterol synthesis and homeostasis are reduced significantly in the brains of *Abcg1*$^{-/-}$ mice compared with their wild-type littermates. Altered gene expression is less pronounced in the brains of *Abcg4*$^{-/-}$ mice, because only farnesyl diphosphate synthase and the LDL receptor mRNA levels were decreased significantly (Fig. 7B). The brain expression of apoER2, fatty acid synthase (*Fas*), a critical gene involved in fatty acid synthesis, or *Cyp46A* (data not shown) was unchanged, indicating that the loss of ABCG1 or ABCG4 function does not lead to global changes in lipid biosynthetic genes (Fig. 7A, B).

DISCUSSION

In the current study, we demonstrate that, although ABCG1 is widely expressed in many tissues and cell types, coexpression of ABCG1 with ABCG4 is restricted to neurons and astrocytes. In addition, studies with *Abcg4*$^{+/-}$/*nlsLacZ* and *Abcg1*$^{+/-}$/*nlsLacZ* mice fail to identify cells that express ABCG4 in the absence of ABCG1. Based on both β-galactosidase staining of tissue sections and quantification of mRNAs in primary mouse cultures, it is clear that basal expression of both genes is significantly higher in neurons compared with astrocytes. Furthermore, ligand activation of LXR induced the mRNA expression of *Abcg1* to nearly equivalent levels in both neurons and astrocytes but failed to alter the mRNA expression of *Abcg4*. A third major cell type in the brain, the microglia, are derived

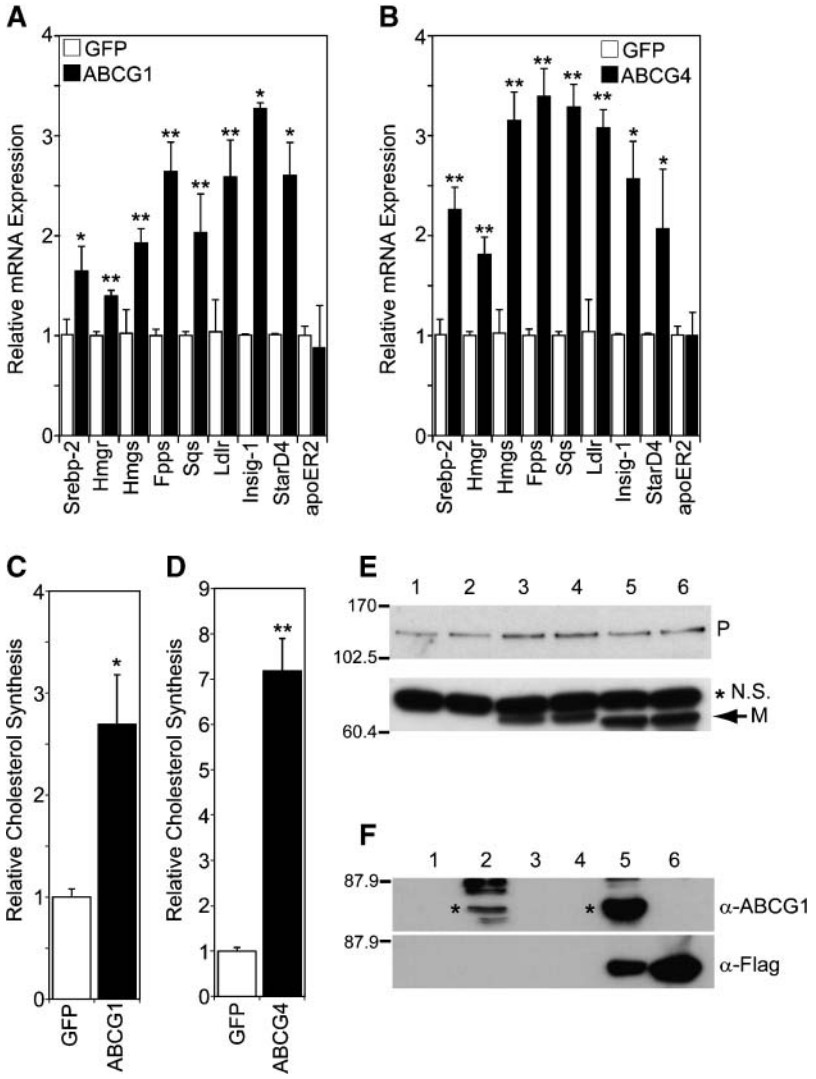

Fig. 5. Expression of ABCG1 or ABCG4 in primary mouse astrocytes increases the mRNA expression of *Srebp-2* and target genes of sterol-regulatory element binding protein 2 (SREBP-2) and cholesterol synthesis. A, B: Duplicate cultures of primary astrocytes were infected with Ad-GFP (open bars), Ad-ABCG1-Flag (closed bars; A), or Ad-ABCG4-Flag (closed bars; B). Gene expression analysis by QPCR shows the upregulation of *Srebp-2* mRNA and its target genes involved in cholesterol synthesis, uptake, and transport. C, D: Cholesterol synthesis, measured by the incorporation of [^{14}C]acetate into cholesterol, is increased significantly in astrocytes infected with adenovirus expressing either ABCG1-Flag (C) or ABCG4-Flag (D). E: Increased levels of both the precursor (P; upper panel) and mature form (M; lower panel, denoted by the arrow) of SREBP-2 after adenoviral expression of ABCG1 (lanes 3, 4) or ABCG4 (lanes 5, 6). Lanes 1 and 2 are the GFP control; note the presence of the precursor form (P) of SREBP-2 (upper panel), whereas the mature form of SREBP-2 is undetectable. The N.S. denoted by the asterisk is a cross-reacting nonspecific band. F: Relative protein levels of ABCG1 (upper panel) in untreated primary astrocytes (lanes 1, 3) or after 1 μM GW3965 treatment for 24 h (lane 2) or after infection with adenovirus expressing GFP (lane 4), ABCG1 (lane 5), or ABCG4 (lane 6). The lower panel demonstrates the relative levels of ABCG1-Flag and ABCG4-Flag after adenoviral expression in primary astrocytes using anti-Flag antibody. The asterisks identify the 78 kDa Flag-tagged ABCG1 or ABCG4. In A–D, the data are representative of two independent experiments and expressed as means ± SEM. * $P < 0.01$, ** $P < 0.001$. In E and F, molecular masses are given in kilodaltons on the left side of the gels.

from circulating monocytes and represent the resident macrophages in this organ. Interestingly, microglia, like human and mouse macrophages, fail to express *Abcg4* mRNA but exhibit significant induction of *Abcg1* after activation of LXR. Together, these data indicate that only neurons and astrocytes express both *Abcg1* and *Abcg4* mRNAs and that *Abcg1*, but not *Abcg4*, is a bona fide LXR target gene.

Immunolocalization studies indicate that ABCG4 and ABCG1 colocalize to intracellular RhoB-positive vesicles.

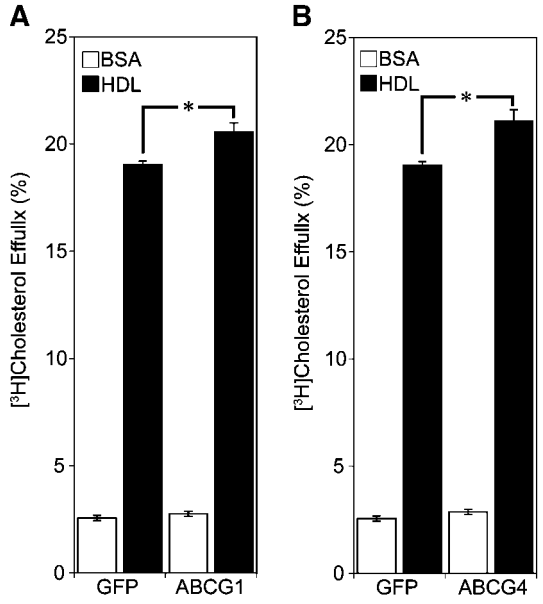

Fig. 6. Expression of ABCG1 (A) and ABCG4 (B) in primary mouse astrocytes increases cholesterol efflux. Quadruplicate dishes of primary mouse astrocytes were infected with adenovirus expressing GFP, ABCG1-Flag, or ABCG4-Flag, as indicated. After infection, astrocytes were incubated with [^{3}H]cholesterol (2 μCi/ml) for 24 h, and [^{3}H]cholesterol efflux to either 0.2% BSA (open bars) or 50 μg/ml human HDL (closed bars) was determined over a 4 h period, as described (20). The data are given as means ± SEM (n = 4). * $P < 0.05$.

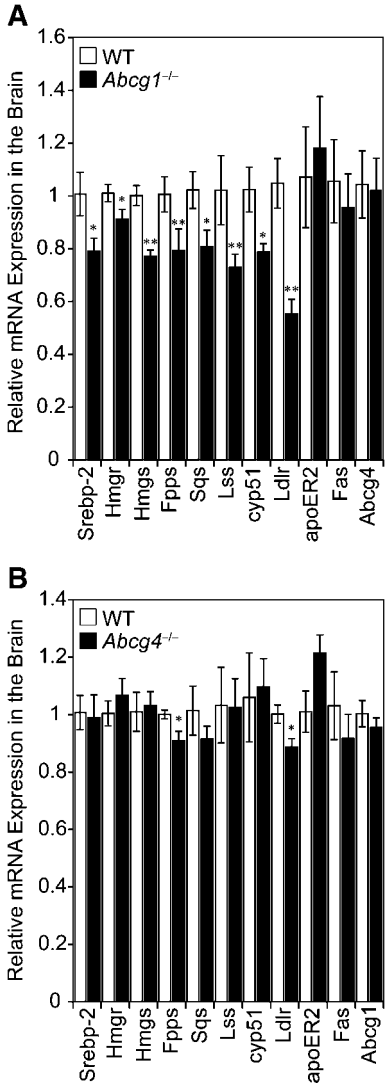

Fig. 7. Decreased expression of genes involved in cholesterol metabolism in the brains of *Abcg1*$^{-/-}$ and *Abcg4*$^{-/-}$ mice. RNA was isolated from the brains of 2 month old chow-fed wild-type (n = 6), *Abcg1*$^{-/-}$ (n = 7) (A), and *Abcg4*$^{-/-}$ (n = 5) (B) mice, and the expression of genes involved in cholesterol homeostasis was quantified by QPCR. *Hmgr*, HMG-CoA reductase; *Hmgs*, HMG-CoA synthase; *Fpps*, farnesyl diphosphate synthase; *Sqs*, squalene synthase; *Ldlr*, low density lipoprotein receptor; *apoER2*, apolipoprotein ER2; *Fas*, fatty acid synthase; Lss, lanosterol synthase. All samples were normalized to GAPDH. Values are given as means ± SEM. * $P < 0.01$, ** $P < 0.001$.

Furthermore, adenoviral expression of either ABCG1 or ABCG4 in primary mouse astrocytes increased the level of the processed nuclear SREBP-2, thereby activating the transcription of numerous target genes that include *StarD4*, *Insig-1*, and many of the genes involved in cholesterol synthesis.

To our knowledge, previous studies have not linked the overexpression of either ABCG1 or ABCG4 to changes in SREBP-2 activation or increased SREBP-2 target gene expression. Importantly, we show that many of the same genes that are induced in primary cells after overexpression of ABCG1 are repressed in the brains of *Abcg1*$^{-/-}$ mice (Fig. 7). The finding that in the brains of *Abcg4*$^{-/-}$ mice the repression of SREBP-2 target genes is less pronounced suggests that ABCG1 may have a more critical role in regulating cholesterol homeostasis in the cells of the CNS.

The regulation of SREBP-2 processing has been elucidated in a series of elegant studies published by Goldstein, DeBose-Boyd, and Brown (34). These investigators have shown that when sterol levels are increased in the endoplasmic reticulum, SREBP-2 is retained in this compartment as a result of the formation of a SREBP/SCAP/INSIG complex. Conversely, depletion of sterols from the endoplasmic reticulum destabilizes the interaction between SCAP and INSIG, allowing the SREBP-2/SCAP complex to be transported to the Golgi in COPII vesicles. After sequential cleavage of the precursor SREBP-2 in the Golgi by two different proteases, the mature, soluble, N-terminal fragment of SREBP-2 translocates to the nucleus, where it activates target genes involved in cholesterol synthesis and uptake (34).

The data in Fig. 5 show clearly that SREBP-2 processing is increased after overexpression of either ABCG4 or ABCG1, consistent with a decrease in sterol levels in the endoplasmic reticulum. Whether ABCG1 and ABCG4 function directly at the endoplasmic reticulum or cause an increase in the transport of cholesterol from the endoplasmic reticulum to vesicles of the endocytic pathway through additional proteins such as StarD4 will require further study. However, the current studies demonstrate

that ABCG1 and ABCG4 are able to regulate SREBP-2 processing and cholesterol synthesis and to promote cholesterol efflux to HDL from within an endocytic compartment (Figs. 3–6).

There are several explanations for how ABCG1 or ABCG4, which localize to intracellular vesicles, can promote the efflux of cholesterol at the plasma membrane to exogenous sterol acceptors. One possibility is that the increase in cholesterol efflux from cells is the result of the endocytic recycling of cholesterol from intracellular membranes back to the plasma membrane, a process known to occur in part by an ATP-dependent vesicular process (35) (**Fig. 8**). Alternatively, efflux may be a result of the direct transport of sterol to the plasma membrane from either the endoplasmic reticulum or another cellular compartment (35). Nonetheless, an earlier study demonstrated that overexpression of ABCG1 in baby hamster kidney cells led to an increase in the cholesterol content of the plasma membrane (19). That study lends support to the idea that some portion of the cholesterol transport mediated by ABCG1 can reach the plasma membrane, where it may desorb to a broad array of exogenous sterol acceptors that include HDL, LDL, phospholipid vesicles, or phospholipid vesicles containing either apoE or apoA-I (9, 10, 15, 16, 18, 25), but not to lipid-poor apoA-I (10, 15). The finding that multiple diverse acceptors function to remove cholesterol from cells in an ABCG1-dependent process is consistent with the desorption of sterol from the plasma membrane to these lipid acceptors. However, we cannot exclude the possibility that some very small fraction of ABCG1 or ABCG4, which is below the level of detection, is localized at the plasma membrane of astrocytes or neurons. Interestingly, studies with non-CNS-derived cells have reported that ABCG1 protein is localized only to intracellular membranes (12, 18) or to both intracellular membranes and the plasma membrane (14, 17, 19).

Support for the importance of ABCG1 or ABCG4 in the regulation of cholesterol homeostasis in the brain is provided by the in vivo findings that many of the genes involved in cholesterol synthesis and transport are repressed in the brains of *Abcg1*$^{-/-}$ and, to a lesser extent, *Abcg4*$^{-/-}$ mice (Fig. 7). Repression of many of these same genes has also been shown to occur in the brains of *Cyp46A*$^{-/-}$ mice.

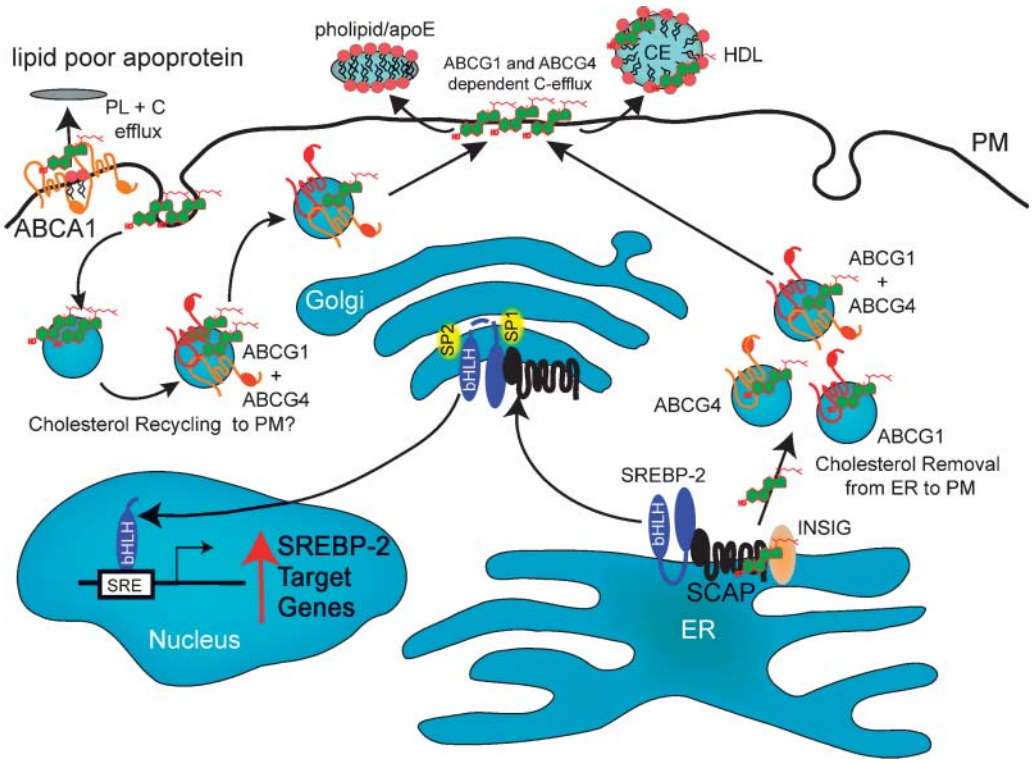

Fig. 8. ABCG1 and ABCG4 regulate the intracellular vesicular transport of cholesterol in neurons and astrocytes. The model shows the presence of ABCG1 and ABCG4 in intracellular vesicles that function to facilitate cholesterol transport from the endoplasmic reticulum to the plasma membrane, where it is available for efflux to exogenous sterol acceptors such as HDL or lipidated apoE. ABCA1 facilitates the efflux of cholesterol (C) and phospholipid (PL) to lipid-poor apolipoproteins. We propose that increased expression of either ABCG1 or ABCG4 results in a decrease in the cholesterol content of the endoplasmic reticulum, with a resulting increase in the processing of SREBP-2 in the Golgi. Subsequent nuclear localization of the mature SREBP-2 increases the transcription of SREBP-2 target genes. ABCG1 or ABCG4 may also regulate the recycling of cholesterol at the cell surface. bHLH, basic helix-loop-helix; CE, cholesteryl ester; ER, endoplasmic reticulum; PM, plasma membrane.

These mice are unable to synthesize 24-hydroxycholesterol from cholesterol and thus are defective in one pathway necessary for the efflux of sterols from the brain into the blood (36). However, *Cyp46A* mRNA levels are unchanged in the brains of *Abcg4*$^{-/-}$ and *Abcg1*$^{-/-}$ mice, suggesting that this enzyme does not play a role in the observed phenotype noted in the current study.

Based on the current studies, we propose that there are two pathways that control intracellular vesicular cholesterol transport in the CNS: the ABCG1-dependent pathway, which is regulated by LXR and thus is responsive to changes in cellular cholesterol content through the production of oxysterol ligands for LXR; and the ABCG4-dependent pathway, which is constitutive and is unresponsive to LXR (Fig. 8). Studies with *Abcg1*$^{-/-}$/*Abcg4*$^{-/-}$ double knockout mice will be required to further assess the overall importance of both transporters in regulating cholesterol homeostasis in the CNS.

The authors thank Dr. Dean Bok at the University of California, Los Angeles for providing human retina RNA for QPCR analysis and Dr. Noam Zelcer at the University of California, Los Angeles for help with astrocyte cultures. The authors thank Dee Bojanic for QPCR analysis of human macrophages and retina. P.T.T. was supported by a National Institutes of Health Predoctoral Fellowship (National Heart, Lung, and Blood Institute Award T32 69766). This work was supported by National Institutes of Health Grants NIH-30568 and NIH-68445 (to P.A.E.), by a grant from the Laubisch Fund, and by an HDL Pfizer Award (to P.A.E.).

REFERENCES

1. Higgins, C. F. 1992. ABC transporters: from microorganisms to man. *Annu. Rev. Cell Biol.* **8:** 67–113.
2. Dean, M., Y. Hamon, and G. Chimini. 2001. The human ATP-binding cassette (ABC) transporter superfamily. *J. Lipid Res.* **42:** 1007–1017.
3. Croop, J. M., G. E. Tiller, J. A. Fletcher, M. L. Lux, E. Raab, D. Goldenson, D. Son, S. Arciniegas, and R. L. Wu. 1997. Isolation and characterization of a mammalian homolog of the Drosophila white gene. *Gene.* **185:** 77–85.
4. Chen, H., C. Rossier, M. D. Lalioti, A. Lynn, A. Chakravarti, G. Perrin, and S. E. Antonarakis. 1996. Cloning of the cDNA for a human homologue of the Drosophila white gene and mapping to chromosome 21q22.3. *Am. J. Hum. Genet.* **59:** 66–75.
5. Savary, S., F. Denizot, M. Luciani, M. Mattei, and G. Chimini. 1996. Molecular cloning of a mammalian ABC transporter homologous to Drosophila white gene. *Mamm. Genome.* **7:** 673–676.
6. Annilo, T., J. Tammur, A. Hutchinson, A. Rzhetsky, M. Dean, and R. Allikmets. 2001. Human and mouse orthologs of a new ATP-binding cassette gene, ABCG4. *Cytogenet. Cell Genet.* **94:** 196–201.
7. Yoshikawa, M., H. Yabuuchi, A. Kuroiwa, Y. Ikegami, Y. Sai, I. Tamai, A. Tsuji, Y. Matsuda, H. Yoshida, and T. Ishikawa. 2002. Molecular and cytogenetic characterization of the mouse ATP-binding cassette transporter Abcg4. *Gene.* **293:** 67–75.
8. Oldfield, S., C. Lowry, J. Ruddick, and S. Lightman. 2002. ABCG4: a novel human white family ABC-transporter expressed in the brain and eye. *Biochim. Biophys. Acta.* **1591:** 175–179.
9. Nakamura, K., M. A. Kennedy, A. Baldan, D. D. Bojanic, K. Lyons, and P. A. Edwards. 2004. Expression and regulation of multiple murine ATP-binding cassette transporter G1 mRNAs/isoforms that stimulate cellular cholesterol efflux to high density lipoprotein. *J. Biol. Chem.* **279:** 45980–45989.
10. Kennedy, M. A., G. C. Barrera, K. Nakamura, A. Baldan, P. Tarr, M. C. Fishbein, J. Frank, O. L. Francone, and P. A. Edwards. 2005. ABCG1 has a critical role in mediating cholesterol efflux to HDL and preventing cellular lipid accumulation. *Cell Metab.* **1:** 121–131.
11. Engel, T., S. Lorkowski, A. Lueken, S. Rust, B. Schluter, G. Berger, P. Cullen, and G. Assmann. 2001. The human ABCG4 gene is regulated by oxysterols and retinoids in monocyte-derived macrophages. *Biochem. Biophys. Res. Commun.* **288:** 483–488.
12. Klucken, J., C. Buchler, E. Orso, W. E. Kaminski, M. Porsch-Ozcurumez, G. Liebisch, M. Kapinsky, W. Diederich, W. Drobnik, M. Dean, et al. 2000. ABCG1 (ABC8), the human homolog of the Drosophila white gene, is a regulator of macrophage cholesterol and phospholipid transport. *Proc. Natl. Acad. Sci. USA.* **97:** 817–822.
13. Venkateswaran, A., J. J. Repa, J. M. Lobaccaro, A. Bronson, D. J. Mangelsdorf, and P. A. Edwards. 2000. Human white/murine ABC8 mRNA levels are highly induced in lipid-loaded macrophages. A transcriptional role for specific oxysterols. *J. Biol. Chem.* **275:** 14700–14707.
14. Wang, N., M. Ranalletta, F. Matsuura, F. Peng, and A. R. Tall. 2006. LXR-induced redistribution of ABCG1 to plasma membrane in macrophages enhances cholesterol mass efflux to HDL. *Arterioscler. Thromb. Vasc. Biol.* **26:** 1310–1316.
15. Wang, N., D. Lan, W. Chen, F. Matsuura, and A. R. Tall. 2004. ATP-binding cassette transporters G1 and G4 mediate cellular cholesterol efflux to high-density lipoproteins. *Proc. Natl. Acad. Sci. USA.* **101:** 9774–9779.
16. Vaughan, A. M., and J. F. Oram. 2006. ABCA1 and ABCG1 or ABCG4 act sequentially to remove cellular cholesterol and generate cholesterol-rich HDL. *J. Lipid Res.* **47:** 2433–2443.
17. Kobayashi, A., Y. Takanezawa, T. Hirata, Y. Shimizu, K. Misasa, N. Kioka, H. Arai, K. Ueda, and M. Matsuo. 2006. Efflux of sphingomyelin, cholesterol, and phosphatidylcholine by ABCG1. *J. Lipid Res.* **47:** 1791–1802.
18. Gelissen, I. C., M. Harris, K. A. Rye, C. Quinn, A. J. Brown, M. Kockx, S. Cartland, M. Packianathan, L. Kritharides, and W. Jessup. 2006. ABCA1 and ABCG1 synergize to mediate cholesterol export to apoA-I. *Arterioscler. Thromb. Vasc. Biol.* **26:** 534–540.
19. Vaughan, A. M., and J. F. Oram. 2005. ABCG1 redistributes cell cholesterol to domains removable by high density lipoprotein but not by lipid-depleted apolipoproteins. *J. Biol. Chem.* **280:** 30150–30157.
20. Baldan, A., P. Tarr, C. S. Vales, J. Frank, T. K. Shimotake, S. Hawgood, and P. A. Edwards. 2006. Deletion of the transmembrane transporter ABCG1 results in progressive pulmonary lipidosis. *J. Biol. Chem.* **281:** 29401–29410.
21. Tachikawa, M., M. Watanabe, S. Hori, M. Fukaya, S. Ohtsuki, T. Asashima, and T. Terasaki. 2005. Distinct spatio-temporal expression of ABCA and ABCG transporters in the developing and adult mouse brain. *J. Neurochem.* **95:** 294–304.
22. Fujiyoshi, M., S. Ohtsuki, S. Hori, M. Tachikawa, and T. Terasaki. 2007. 24S-Hydroxycholesterol induces cholesterol release from choroid plexus epithelial cells in an apical- and apoE isoform-dependent manner concomitantly with the induction of ABCA1 and ABCG1 expression. *J. Neurochem.* **100:** 968–978.
23. Karten, B., R. B. Campenot, D. E. Vance, and J. E. Vance. 2006. Expression of ABCG1, but not ABCA1, correlates with cholesterol release by cerebellar astroglia. *J. Biol. Chem.* **281:** 4049–4057.
24. Abildayeva, K., P. J. Jansen, V. Hirsch-Reinshagen, V. W. Bloks, A. H. Bakker, F. C. Ramaekers, J. de Vente, A. K. Groen, C. L. Wellington, F. Kuipers, et al. 2006. 24(S)-Hydroxycholesterol participates in a liver X receptor-controlled pathway in astrocytes that regulates apolipoprotein E-mediated cholesterol efflux. *J. Biol. Chem.* **281:** 12799–12808.
25. Kim, W. S., A. S. Rahmanto, A. Kamili, K. A. Rye, G. J. Guillemin, I. C. Gelissen, W. Jessup, A. F. Hill, and B. Garner. 2007. Role of ABCG1 and ABCA1 in regulation of neuronal cholesterol efflux to apolipoprotein E discs and suppression of amyloid-beta peptide generation. *J. Biol. Chem.* **282:** 2851–2861.
26. Tansley, G. H., B. L. Burgess, M. T. Bryan, Y. Su, V. Hirsch-Reinshagen, J. Pearce, J. Y. Chan, A. Wilkinson, J. Evans, K. E. Naus, et al. 2007. The cholesterol transporter ABCG1 modulates the subcellular distribution and proteolytic processing of beta-amyloid precursor protein. *J. Lipid Res.* **48:** 1022–1034.
27. Saura, J., J. M. Tusell, and J. Serratosa. 2003. High-yield isolation of murine microglia by mild trypsinization. *Glia.* **44:** 183–189.
28. Radhakrishnan, A., Y. Ikeda, H. J. Kwon, M. S. Brown, and J. L. Goldstein. 2007. Sterol-regulated transport of SREBPs from

endoplasmic reticulum to Golgi: oxysterols block transport by binding to Insig. *Proc. Natl. Acad. Sci. USA.* **104:** 6511–6518.
29. Vance, J. E., B. Karten, and H. Hayashi. 2006. Lipid dynamics in neurons. *Biochem. Soc. Trans.* **34:** 399–403.
30. Whitney, K. D., M. A. Watson, J. L. Collins, W. G. Benson, T. M. Stone, M. J. Numerick, T. K. Tippin, J. G. Wilson, D. A. Winegar, and S. A. Kliewer. 2002. Regulation of cholesterol homeostasis by the liver X receptors in the central nervous system. *Mol. Endocrinol.* **16:** 1378–1385.
31. Baldan, A., P. Tarr, R. Lee, and P. A. Edwards. 2006. ATP-binding cassette transporter G1 and lipid homeostasis. *Curr. Opin. Lipidol.* **17:** 227–232.
32. Fernandez-Borja, M., L. Janssen, D. Verwoerd, P. Hordijk, and J. Neefjes. 2005. RhoB regulates endosome transport by promoting actin assembly on endosomal membranes through Dia1. *J. Cell Sci.* **118:** 2661–2670.
33. Sun, L. P., L. Li, J. L. Goldstein, and M. S. Brown. 2005. Insig required for sterol-mediated inhibition of Scap/SREBP binding to COPII proteins in vitro. *J. Biol. Chem.* **280:** 26483–26490.
34. Goldstein, J. L., R. A. DeBose-Boyd, and M. S. Brown. 2006. Protein sensors for membrane sterols. *Cell.* **124:** 35–46.
35. Maxfield, F. R., and I. Tabas. 2005. Role of cholesterol and lipid organization in disease. *Nature.* **438:** 612–621.
36. Lund, E. G., C. Xie, T. Kotti, S. D. Turley, J. M. Dietschy, and D. W. Russell. 2003. Knockout of the cholesterol 24-hydroxylase gene in mice reveals a brain-specific mechanism of cholesterol turnover. *J. Biol. Chem.* **278:** 22980–22988.